fire

MDPI

Article

Effect of Initial Temperature on Flame Spread over a Sand Bed Wetted with Transformer Oil

Jiaqing Zhang [1,2,3,*], Yubiao Huang [1,2,3,*], Yi Guo [1,2,3] and Guocheng Ding [1,2,3]

[1] State Grid Anhui Electric Power Research Institute, Hefei 230601, China; gy524635748@163.com (Y.G.); cyf1990123@163.com (G.D.)
[2] State Grid Laboratory of Fire Protection for Transmission and Distribution Facilities, Hefei 230601, China
[3] Anhui Provincial Key Laboratory of New Type Power Systems Fire Safety and Emergency Technology, Hefei 230601, China
* Correspondence: dkyzjq@163.com (J.Z.); firelab_huang@163.com (Y.H.)

Abstract: A series of experiments were conducted on quartz sand beds wetted with transformer oil under initial temperatures of 80–140 °C and fuel–sand mass ratios of 1:4–1:8. The flame spreading process over the fine sand bed wetted with limited liquid fuel can be divided into the development and quasi-steady stages. Experimental results reveal that the flame spread rate in the quasi-steady stage increases with the initial temperature and fuel–sand mass ratio. The effect of sand bed width on flame spread depends on the initial temperature. The flame spread rate is insensitive to the sand bed width at low initial temperatures; however, it increases with sand bed width at an initial temperature close to the flash point of liquid fuel. This discrepancy mainly results from the enhanced capillary effect due to the decreased viscosity at high initial temperatures. The capillary effect is the dominant factor determining fuel vaporization and, thus, the flame spread rate, and flame radiation plays an increasing role with increasing initial temperature. The maximum flame height is sensitive to sand bed width and fuel–sand mass ratio but changes little with initial temperature. A dimensionless model was proposed to predict the normalized flame height.

Keywords: flame spread; transformer oil; sand bed; initial temperature; flame height

Academic Editor: Thomas H. Fletcher

Received: 10 April 2025
Revised: 5 May 2025
Accepted: 8 May 2025
Published: 10 May 2025

Citation: Zhang, J.; Huang, Y.; Guo, Y.; Ding, G. Effect of Initial Temperature on Flame Spread over a Sand Bed Wetted with Transformer Oil. *Fire* **2025**, *8*, 193. https://doi.org/10.3390/fire8050193

1. Introduction

The spillage accidents of flammable liquids from damage to storage tanks and equipment periodically occur [1–3]. The flammable liquid may penetrate into porous media, such as concrete slabs and sand beds [4,5]. If the fuel is ignited, subsequently, flame spread over the porous bed surface would be severe since the porous bed may play the role of a wick [6]. The flame spread behavior over porous beds wetted with liquid fuel are different from those of pool fires. Therefore, flame spread over porous media wetted with liquid fuels with various flash points (T_{fla}) has been extensively investigated to understand the potential secondary fire accidents after the spillage of combustible liquid [7–9].

The sand size, initial amount of fuel (or fuel–sand mass ratio), and sand bed depth are the most extensively investigated factors influencing the flame spread behaviors over porous media wetted with liquid fuel. With increasing sand size, both the flame spread rate and burning rate decrease due to the reduced capillary rise effect [10]. When sand size exceeds a critical threshold, the flame extinguishes gradually. For both liquid pools and the sand beds wetted with liquid, the flame spread rate increases with the initial temperature when it is below the flash point [8,11]. Once the initial temperature exceeds the flash point, the flame spread rate becomes independent of the initial temperature.

The fuel–sand mass ratio, which is defined as the proportion of liquid fuel to sand particles, significantly affects the flame spread behaviors. Fu et al. [12] conducted experiments on flame spread over diesel-wetted sand beds (0.15–0.4 L/kg) and observed a direct correlation between fuel content and flame spread rate. At low fuel–sand mass ratios, flame spread is primarily controlled by capillary rise and sand bed heat conduction, whereas radiative heat transfer dominates at higher fuel–sand mass ratios. In addition, a decreasing bed depth enhances flame spread, while initiation delay amplifies the vapor phase's role in the flame spread over sand wetted with 2-propanol [13].

The flame spread mechanism over sand beds wetted with liquid fuel under quiescent and windy conditions has been investigated [14–17]. For kerosene-wetted sand under varying initial temperatures, opposed airflow was observed to shift the dominant flame spread mechanism. The flame spread is dominated by flame radiation in a quiescent atmosphere; however, it is governed by heat conduction through the sand layer under opposed wind conditions [14]. The effect of concurrent flow on the flame spread over wetted sand beds was investigated by Ishida [15]. The flame spread process was steady in concurrent flow and was determined primarily by the formation of flammable gas mixtures at the leading edge. Further analysis of propanol-wetted sand beds under wind showed that the normalized flame spread rate by the rate at quiescent conditions correlates strongly with the Damköhler number (Da) [17].

While flame spread behavior over liquid fuel-wetted sand beds is known to depend on fuel properties, the existing literature predominantly focuses on highly volatile liquids with low flash points (lower than ambient temperature). Data of flame spread over weakly volatile liquids (with high flash points) are scarce. However, fire accidents may happen when these liquids spill over porous media at high initial temperatures. The present study aims to explore the flame spread behavior over sand beds wetted with weakly volatile liquid fuel. The 25# transformer oil, which is a liquid widely used as an insulating and cooling medium in oil-immersed transformers [18–22], was selected as the liquid fuel. This oil has a flash point of approximately 145 °C [23]. Fine quartz sand with an average diameter of 0.32 mm was employed as the porous substrate. The effects of sand bed width, initial temperature, and fuel–sand mass ratio on flame spread rate and flame height over sand bed wetted with 25# transformer oil were systematically analyzed. Based on thermal equilibrium analysis in the preheat region, the influencing mechanisms of the above factors on flame spread rate were revealed. Additionally, a dimensionless model was developed to predict flame height during quasi-steady spreading phases. The results help to understand the influencing mechanism of initial temperature on flame spread over porous solids wetted with weakly volatile liquids and provide insights for preventing accidental fire spread in electronic transformer stations.

2. Experimental Setup

Figure 1 illustrates the schematic diagram of the experimental setup. The Karamay 25# transformer oil (Kunlun KI25X) and quartz sand were weighed and prepared with a mass ratio (r) of 1:4, 1:6, and 1:8. Quartz glassware with a length (L) of 250 mm, depth (δ) of 8 mm, and widths (W) of 25 mm, 50 mm, and 100 mm were used to hold the quartz sand wetted with liquid. The sand bed surface was kept flush with the quartz glassware. The wetted sand bed was heated by an electric heater and the temperature of the heater could be adjusted. As the temperature of the wetted sand reached the set temperature (T_0), ranging from 80 °C to 140 °C, the electric heating wire (60 W) positioned near the glassware's end was turned on. The ignition delay time was nearly independent of sand bed width but mildly decreased with increasing sand bed temperature. After ignition, the electric heating wire was turned off immediately to reduce the preheating effects.

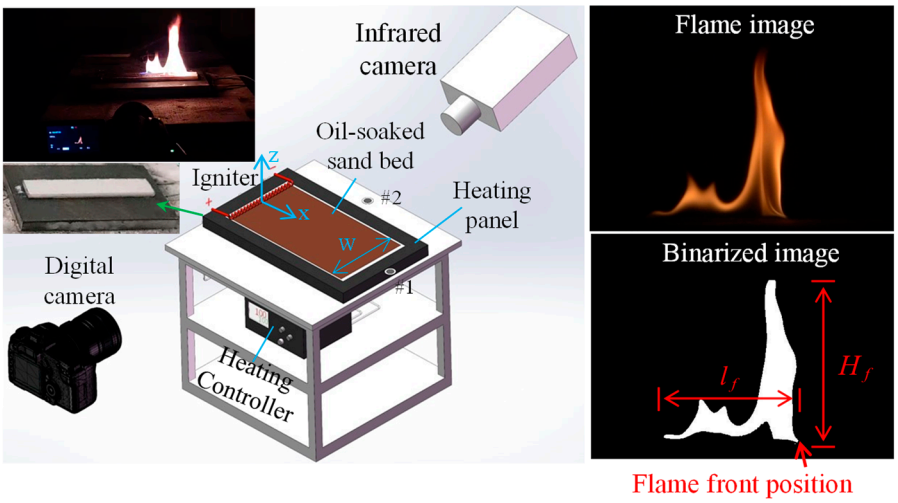

Figure 1. Experimental setup and the definitions of flame height and the length of the burning region.

The temperature of the sand bed surface was recorded by an infrared camera (IR, with a wavelength of 8–14 μm). Two Schmidt-Boelter radiometers (water-cooled, measurement range of 50 kW/m^2, repeatability of 0.5%) were positioned at the glassware's geometric center along both the length and width axes, separated by 30 mm. A SONY camera (AX-700, with an effective resolution of 1920 × 1080 pixels and a frame rate of 100 fps), was mounted 1.5 m from the platform to capture the flame spread process. The frames at 10 s intervals were taken from the recorded video and were processed using Otsu's method [24]. The flame front position, maximum flame height (H_f), and the length of the burning region (l_f) of each frame can be obtained, as shown in Figure 1. To ensure the reliability of the experimental results, all experiments (as shown in Table 1) were repeated at least three times.

Table 1. Summary of experimental conditions.

Sand Bed Width, W (mm)	Sand Bed Depth, δ (mm)	Sand Bed Length, L (mm)	Fuel–Sand Mass Ratio, r	Initial Temperature, T_0 (°C)
25, 50, 100	8	250	1:4, 1:6, 1:8	80, 100, 120, 140

3. Results and Discussion

3.1. Flame Spread Process over Sand Bed Wetted with Transformer Oil

Figure 2 shows the image sequences for flame spread over a 50 mm width fuel bed at four different initial temperatures. Under different conditions, the length of the burning region and maximum flame height initially increase and stabilize gradually, indicating a transition to a steady-state regime. The fuel bed can be divided into three regions, raw bed, burning region, and burnout region. The length of the burning region in the steady-state stage increases with increasing initial temperature. A periodically pulsating blue flame was observed near the trailing edge of the burning zone. This phenomenon was previously reported in liquid pool fires and vertical plate spill fires [21,25]. The pulsation is attributed to constrained fuel supply near the burnout zone and becomes more pronounced at lower fuel–sand mass ratios. The residual fuel in the burnout zone vaporizes slightly and the flame proceeds backward as the fuel vapor concentration attains the lean flammability limit. Then, the fuel vapor is consumed rapidly and, therefore, the flame proceeds forward. At large fuel–sand mass ratios, the fuel supply is enhanced due to the capillary effect and a stable flame is more likely to be formed. In addition, flames at T_0 = 140 °C exhibited enhanced yellow luminosity compared to lower initial temperature conditions,

indicative of intensified combustion and higher fuel vapor oxidation efficiency at elevated initial temperatures [26].

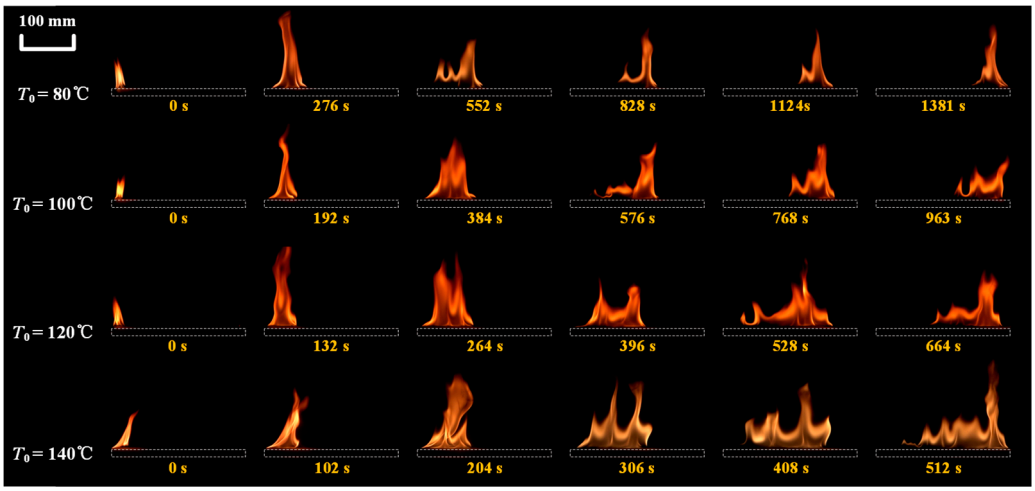

Figure 2. Image sequences for flame spread over a sand bed with a fuel–sand mass ratio of 1:4 and at 4 different initial temperatures.

From the recorded video, the flame height and the length of the burning region were measured. Figure 3 shows the variations of flame height (black symbols) and the length of the burning region (red symbols) with time after ignition for flame spread over 100 mm wide sand beds at four different initial temperatures. At $T_0 \leq 100$ °C, the flame height increases to a peak value followed by abrupt reduction before reaching a steady state. The length of the burning region exhibits a temporal evolution comparable to that of flame height. However, it requires additional time to reach stabilization, likely due to delayed burnout front propagation. Based on experimental observations, the flame spread at low initial temperatures can be divided into three different stages: development stage, transient stage, and quasi-steady stage. It is interesting to note that the maximum flame height in the development stage exceeds that in the quasi-steady stage at low initial temperatures, which has been found in the burning of sand beds wetted with liquid combustibles [10]. This is mainly due to the larger fuel content and fuel supply rate in the development stage. In the initial stage after ignition, both the flame height and the length of the burning region increase with time, leading to an increased consumption rate of fuel. As the fire grows, the fuel content in the burning region decreases and the upper layer of the fuel bed becomes dry. As a result, the fuel supply is restricted, leading to decreased flame height. The restricted fuel supply and enhanced heat transfer have opposite effects on the burning rate. As the two factors become comparable, the flame height remains unchanged with time. At elevated initial temperatures ($T_0 \geq 120$ °C), the flame height increases gradually and stabilizes at approximately 200 s. Simultaneously, the length of the burning region increases monotonically with time, indicating enhanced fuel supply under elevated initial temperatures. This phenomenon primarily arises from the decreased viscosity of transformer oil at a larger temperature [27], which increases the capillary effect and fuel supply rate.

Figure 4 shows the diagrams of the diffusion flame and fuel distribution within the sand bed in the development and steady stages. It is preferred that the capillary rise effect plays a great effect on diffusion burning. After ignition, the flame in the burning region increases in size and a quasi-steady stage is finally achieved.

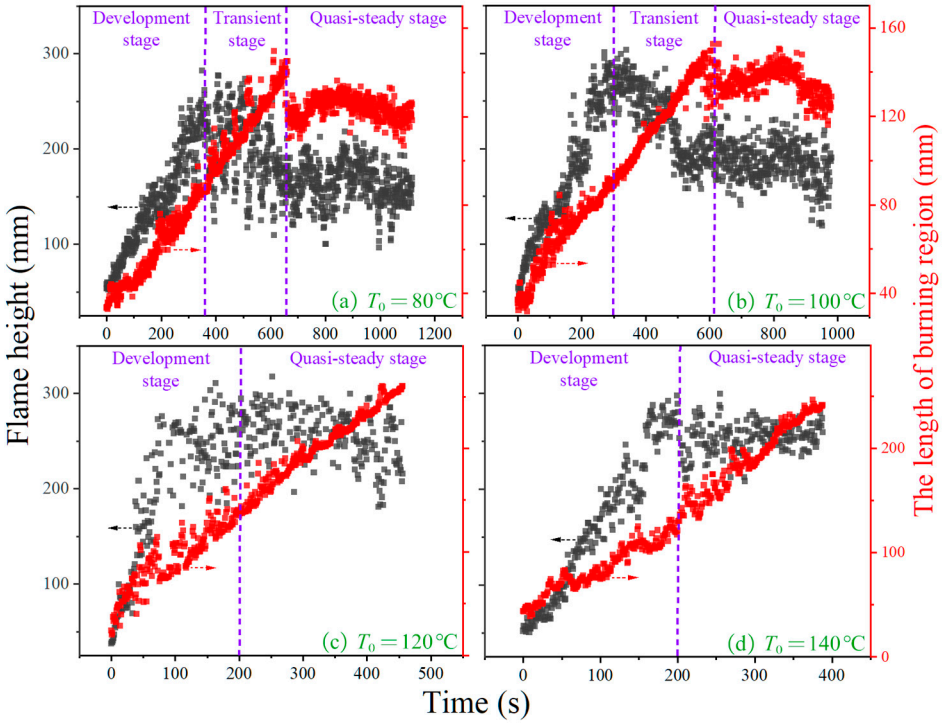

Figure 3. Flame height and the width of burning region versus time at initial temperatures of 80 °C (**a**), 100 °C (**b**), 120 °C (**c**), and 140 °C (**d**) for 100 mm sand bed at a fuel–sand mass ratio of 1:4.

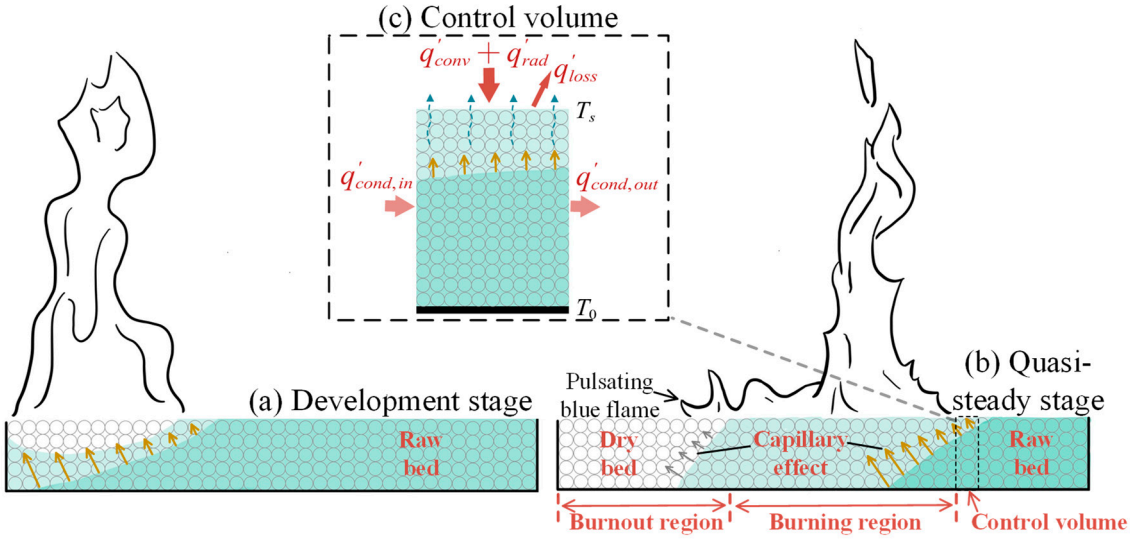

Figure 4. The diagram of flame spread in the development stage (**a**), the quasi-steady stage (**b**), and the control volume in the preheating region (**c**).

Flame spread over a solid surface can be treated as a continuous ignition process [16,17,28]. The energy required to heat the raw fuel-wetted sand bed to the ignitable state (flash point of transformer oil) equals to the energy delivered to the sand bed. Taking the preheating region per unit width (as shown in Figure 4c) as the control volume, the energy balance equation per unit width for flame spread over the fuel bed can be derived, which is shown in Equation (1). The three terms on the left-hand side represent the convective heat flux per unit width (q'_{conv}), the radiative heat flux per unit width (q'_{rad}), and the net heat delivered to the control volume through solid-phase conduction per unit width ($q'_{cond,net}$), respectively. The two terms on the right-hand side quantify the energy required to heat

the control volume from the initial temperature to the ignitable state and the radiative heat loss per unit width (q'_{loss}).

$$k_g \frac{(T_f - T_{fla})}{\delta_g} \delta_l + \varepsilon_a \sigma F ({T_f}^4 - {T_{fla}}^4) L_0 + q'_{cond,net} = \dot{m}'' L_0 (\Delta H_v + c_p (T_{fla} - T_0)) + \varepsilon_e \sigma {T_{fla}}^4 L_0 \quad (1)$$

where δ_g, δ_l, and L_0 are the distance between the flame front and the fuel bed, the characteristic length scale of the convection heating, and the length of the control volume, respectively. T_f is the flame temperature. ε_a, ε_e, σ, and F are the absorptivity, emissivity for the sand bed, Stephen Boltzmann constant, and the view factor, respectively. ΔH_v and c_p are the latent heat of vaporization and the specific heat capacity of transformer oil. Due to the nonuniform distributions of fuel and temperature with the sand bed, it is difficult to evaluate the conductive heat flux accurately. $\dot{m}''$ is the mass flow rate of fuel vapor at the surface of the sand bed and can be treated as a constant.

Due to the conduction through the sand bed and the convective and radiative heat feedback from the diffusion flame, the temperature in the preheating region increases gradually. The liquid fuel in the sand bed is vaporized and then spills from the sand bed surface. Meanwhile, the upper part of the sand bed becomes a dry porous layer without combustible liquid and acts as an "insulation layer", which isolates the radiative and convective heat fluxes as a consequence. As a result, heat conduction through the solid plays a dominant role in vaporizing the fuel within the sand bed [8,29]. When the concentration of gaseous fuels accumulating at the preheating region's surface reaches the lean combustion limit, the sand bed in this region ignites.

3.2. Flame Spread Rate

The flame spread rate can be determined as the derivative of the flame front position with respect to time. Figure 5a–c show the transient flame front position versus time after ignition for fuel beds with different initial temperatures, fuel–sand mass ratios, and widths. It is obvious that the flame front position is nearly linear with time under $T_0 \leq 120$ °C, although small disturbances exist. At $T_0 = 140$ °C, the flame spread shows a slight acceleration tendency. In general, the flame spreads faster at larger initial temperatures or fuel–sand mass ratios. However, the effect of sand bed width on the flame spread depends on the initial temperature, as shown in Figure 5c. At $T_0 = 100$ °C, the flame front position has a similar trend with time, indicating that the flame spread rate is insensitive to the sand bed width. However, the evolution of the flame front varies with the sand bed width at $T_0 = 140$ °C. The flame spreads faster with the increased sand bed width in this condition. This outcome can be explained by reduced fuel viscosity near the flash point, which enhances the capillary effect and fuel supply rate.

The coefficient of determination (R^2) for the linear regression analysis of the flame front position in the quasi-steady stage ranges from 0.92 to 0.99. Figure 6 show the variations of the average flame spread rate with the initial temperature under different conditions. Evidently, the flame spread rate increases with increasing initial temperature for sand beds with different widths and fuel–sand mass ratios. The increasing rate of flame spread rate with initial temperature is more prominent at a larger fuel–sand mass ratio and a higher initial temperature. The energy needed to heat the fuel-wetted sand bed to an ignitable state (corresponding to the first term on the right-hand side of Equation (1)) decreases with increasing initial temperature. The formation of flammable gaseous vapors from transformer oil in the preheating region becomes easier, thereby increasing the flame spread rate. In addition, it is seen that the flame spread rate is nearly independent of the sand bed width at $T_0 \leq 100$ °C, different from the behavior observed for flame spread over

polymers [30,31]. However, when the initial temperature reaches 120 °C (fuel–sand mass ratio 1:4) or 140 °C (ratios 1:6 and 1:8), the sand bed width significantly affects the flame spread rate.

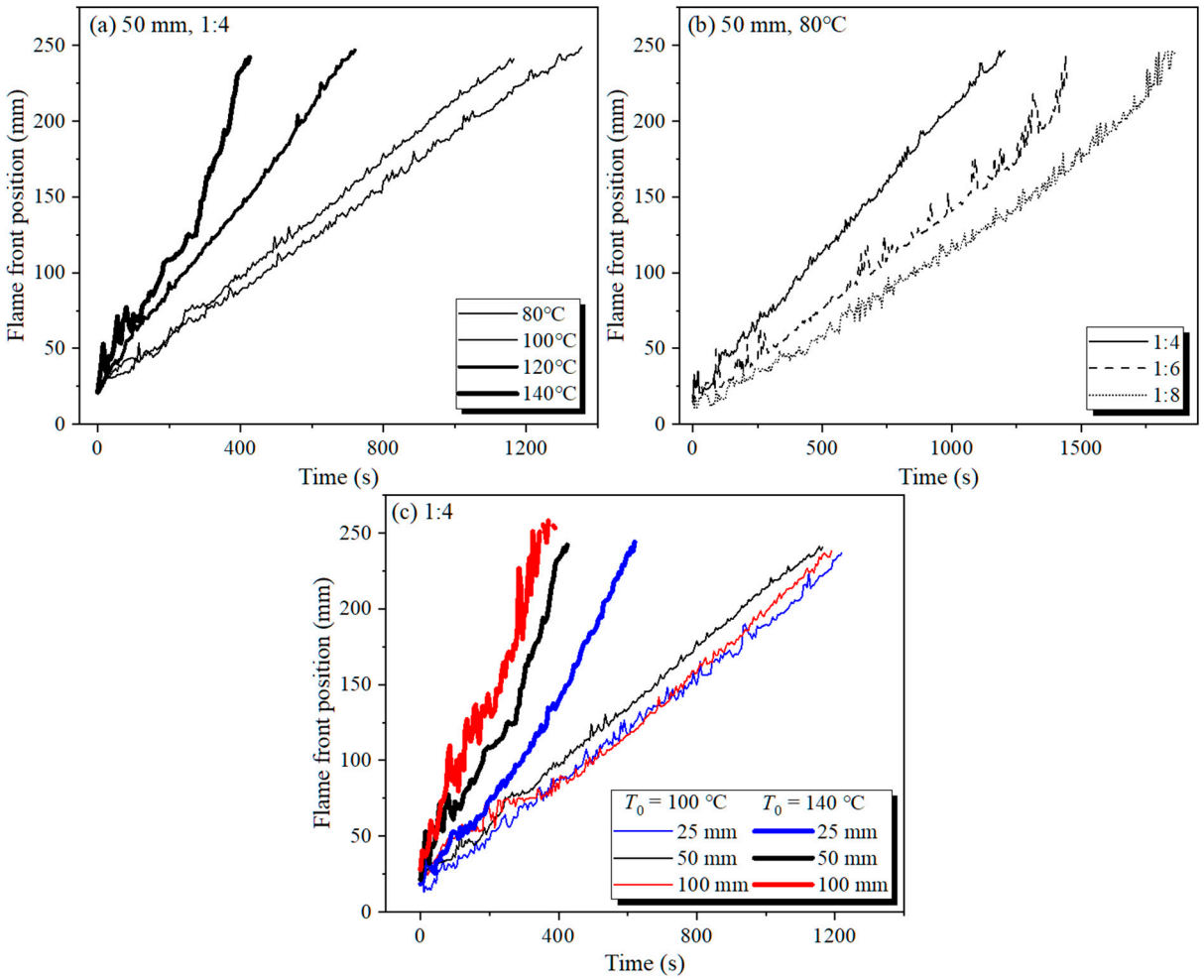

Figure 5. Flame front position versus time under (**a**) various initial temperatures (W = 50 mm, r = 1:4), (**b**) various fuel–sand mass ratios (W = 50 mm, T_0 = 80 °C), and (**c**) various sand bed widths (T_0 = 100 °C and 140 °C, r = 1:4).

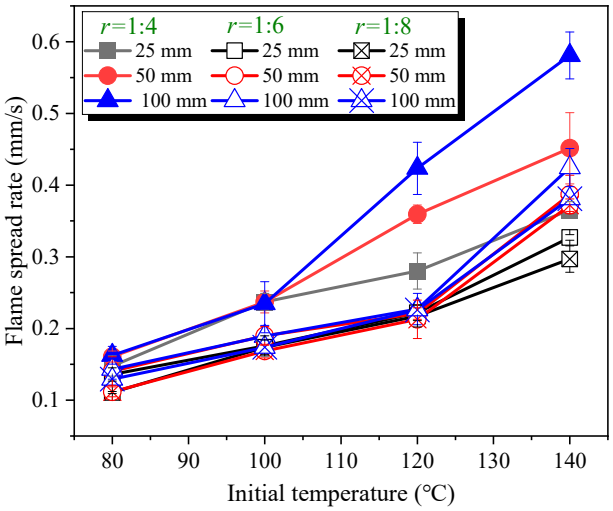

Figure 6. Flame spread rate versus initial temperature of sand bed at different sample widths and fuel–sand mass ratios.

The temperature at the center of the sand bed (obtained from IR videos) and the radiative heat flux measured by the radiometers are given in Figure 7. It is seen that the sand bed surface temperature increases sharply once the temperature exceeds the flash temperature of the transformer oil (145 °C, [23]). The maximum surface temperature remains relatively constant across all tested initial temperatures, whereas radiative heat flux at different positions increases significantly. Elevated initial temperatures correlate with expanded burning zone lengths and flame heights. Consequently, flame emissivity and view factor rise [21,32]. Furthermore, larger flame dimensions at higher initial temperatures intensify radiative heat flux, directly accelerating the flame spread rate. For flame spread over liquid-wetted sand beds, fuel vaporization predominantly occurs near the surface due to localized heating. Lower fuel–sand mass ratios increase the dry sand layer depth, which restricts upward fuel vapor transport. It is preferred that the capillary effect is the dominant factor determining flame spread rate at low initial temperatures. In such cases, the flame spread rate depends primarily on the initial temperature. As temperature rises, reduced transformer oil viscosity strengthens capillary effects, while sand bed width exerts a stronger influence. Wider beds amplify flame height and radiative feedback (via increased emissivity and view factor), leading to faster flame spread under elevated temperatures.

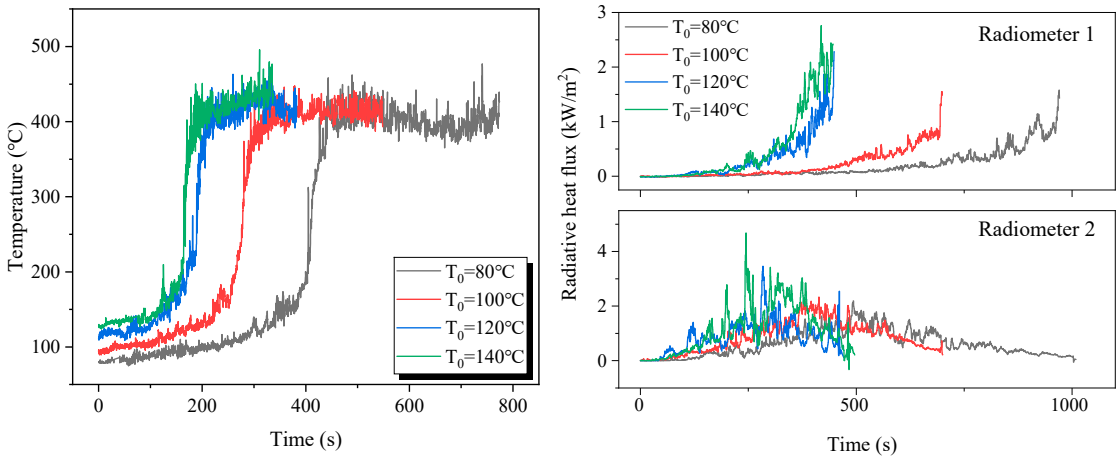

Figure 7. The temperature evolution at the middle of the sand bed and the history of heat flux recorded by two different radiometers for the fuel bed at different initial temperatures.

3.3. Flame Height in the Quasi-Steady Stage

For diffusion flames, the flame extends to the length where the fuel stoichiometric flame is achieved [33]. Flame height, a key parameter in characterizing fire dynamics, is governed by molecular diffusion in laminar flames and air entrainment in turbulent regimes. It was confirmed that flame height closely correlates with the heat release rate (burning rate) for different types of fires [34–36]. Figure 8 shows the variation of flame height in the quasi-steady stage with initial temperature at different sand bed widths and fuel–sand mass ratios. It is seen that the flame height shows a marked rise with increasing sample width and fuel–sand mass ratio. The flame height increases slightly with the initial temperature in most conditions but increases appreciably for the 100 mm width sand bed at a fuel–sand mass ratio of 1:4. This observation indicates that the enhancement effect of elevated temperatures on capillary action progressively intensifies with increasing sand bed width.

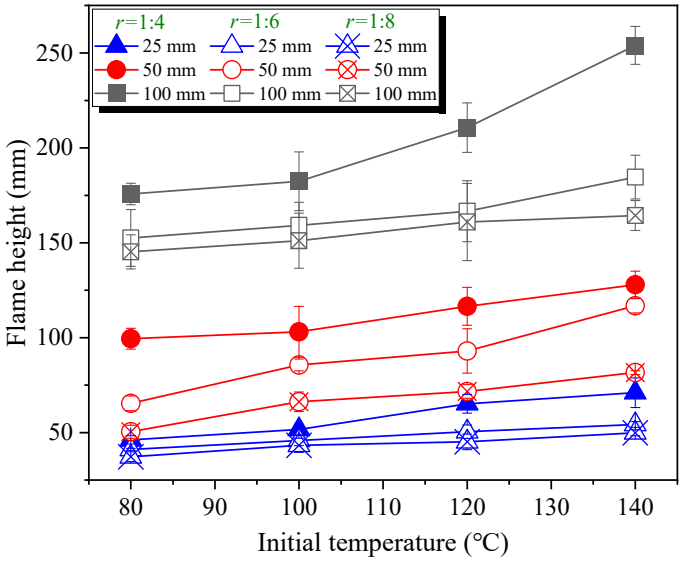

Figure 8. The variation of the flame height in the quasi-steady stage with the initial temperature at different conditions.

In the quasi-steady stage, the mass burning rate is linearly proportional to the flame spread rate [34]:

$$\dot{m} = V_f \delta W \phi \rho_s r \tag{2}$$

where ϕ and ρ_s are the volume porosity and density of dry sand particles, 0.52 and 2650 kg/m^3, respectively. The normalized flame height is often correlated with a dimensionless heat release rate [36–39], which is defined as follows:

$$Q^* = \frac{\dot{m}\Delta H_c}{\rho_\infty T_\infty c_{p,air}\sqrt{gD}D^2} \tag{3}$$

where g, ρ_∞, T_∞, and $c_{p,air}$ are the gravitational acceleration, the density, temperature, and specific heat of air, respectively. ΔH_c is the effective combustion heat of transformer oil, taken as 40 MJ/kg [21]. D is the characteristic length of the fire, taken as the width of the sand bed, since it is the most important parameter influencing the flame height (as shown in Figure 8). Based on a concatenated fitting, the correlation between the normalized flame height (H_f/W) and the dimensionless heat release rate $(\frac{\dot{m}\Delta H_c}{\rho_\infty T_\infty c_{p,air}\sqrt{gW}W^2})$ is formulated as Equation (4).

$$\frac{H_f}{W} = 2.67\left(\frac{\dot{m}\Delta H_c}{\rho_\infty T_\infty c_{p,air}\sqrt{gW}W^2}\right)^{0.17} \tag{4}$$

As shown in Figure 9, the correlation given in Equation (4) coincides well with the experimental results under different conditions. The power is 0.17, much smaller than that for horizontal flame spread over a thin PMMA surface (0.38–0.6) [40] and that of non-spreading pool fires (0.4–1) [1,37,41]). In addition, the exponent of H_f on W in the present study is 0.575, smaller than that for flame spread over a wood sheet (0.725) [42]. In other words, the dependence of flame height on the mass burning rate and sample width is weaker. This discrepancy arises from fundamental differences in combustion behavior and significant difference in fuel supply mechanisms between liquid pool fires and the fires of liquid-wetted sand beds. The maximum flame height is located at the center of the fire source for pool fire but near the flame front for the latter. In other words, flame height in the present study depends on the local mass loss rate near the flame front. The local vaporization rate of liquid fuel is non-uniform and the capillary effect is the most important

factor affecting combustion for sand beds wetted with liquid fuel. Such differences account for the smaller exponent.

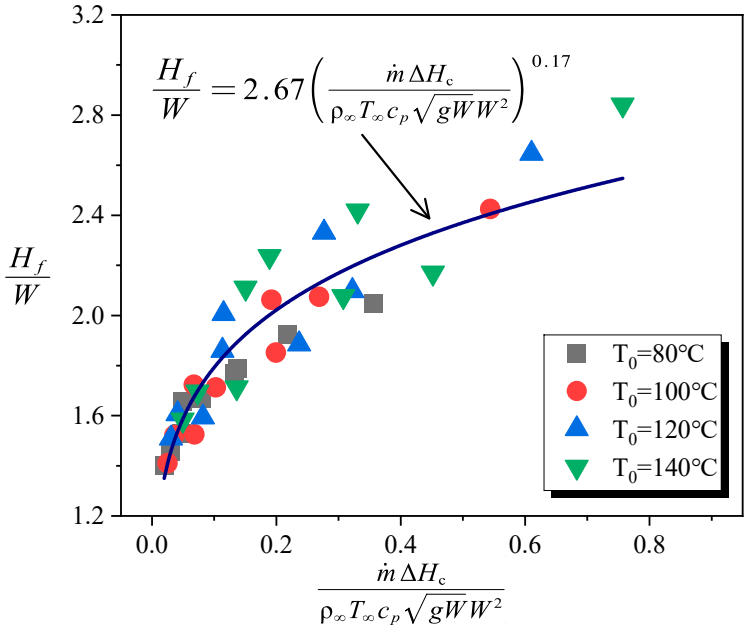

Figure 9. The correlation between the normalized flame height and the dimensionless heat release rate.

4. Conclusions

An experimental study was conducted on flame spread over the fine sand bed wetted with 25# transformer oil at four different initial temperatures. The flame spread rate, flame height, and the length of the burning region were quantified and analyzed in this study. The main findings are as follows:

(1) The flame spread rate over the fine sand bed wetted with transformer oil depends mainly on the fuel–sand mass ratio and initial temperature. At low initial temperatures, the flame spread rate increases with initial temperature and the effect of sand bed width is negligible. Due to the combined effect of enhanced capillary effect and increased heat feedback, width effects become apparent at initial temperatures close to the flash point.

(2) The flame height in the quasi-steady stage is related to the sand bed width and fuel–sand mass ratio but is insensitive to the initial temperature of the sand bed.

(3) An empirical correlation between the normalized flame height and the dimensionless heat release rate is proposed, as given in Equation (4).

Bench-scale experiments were conducted in the present study to investigate the effects of initial temperature on the flame spread behavior over sand beds wetted with 25# transformer oil. The findings and empirical model are applicable to predict the early-stage flame spread behaviors over fine sand beds wetted with liquid fuels. Large-scale experiments are needed to gain deeper insights into the controlling mechanisms of flame spread over the fuel-wetted porous solids.

Author Contributions: J.Z.: Conceptualization, Formal analysis, Writing—original draft preparation, and Funding acquisition; Y.H.: Investigation, Methodology, Writing—review and editing, and Supervision; Y.G.: Investigation and Formal analysis; G.D.: Investigation and Methodology. All authors have read and agreed to the published version of the manuscript.

Funding: This research was funded by State Grid Anhui Electric Power Co., Ltd., grant number B3120523000D (the Science and Technology Project).

Institutional Review Board Statement: Not applicable.

Informed Consent Statement: Not applicable.

Data Availability Statement: The original contributions presented in this study are included in the article. Further inquiries can be directed to the corresponding author.

Conflicts of Interest: The authors declare no conflicts of interest.

References

1. Zhang, Y.; Chen, C. An experimental study on burning characteristics and temperature distribution of inert porous sand bed soaked by leaked combustible liquid. *Int. J. Therm. Sci.* **2022**, *179*, 107594. [CrossRef]
2. Zhao, J.; He, Y.; Xiao, J.; Su, Z.; Ma, H.; Zhai, X. Experimental Investigation of the Spread and Burning Behaviors of Diesel Spill Fires on a Water Surface. *Fire* **2024**, *7*, 402. [CrossRef]
3. Ding, C.; Ma, S.; Yan, Z.; He, L.; Li, Y.; Fang, T.; Jiao, Y. Experimental Study on the Effect of Sub-Flash Point Fuel Temperature on the Spread Characteristics of Spill Fire. *Fire* **2023**, *6*, 284. [CrossRef]
4. Xu, T.; Lei, P. Experimental study on flame height and heat release rate estimation of diesel-wetted wood powder fire. *Case Stud. Therm. Eng.* **2022**, *33*, 101906. [CrossRef]
5. Chen, C.; Lei, P.; Zhang, Y.; Xiao, H.; Xu, T.; Jiao, W. Experimental study of influence of fuel ratio on combustion characteristics of diesel-wetted wood powder. *J. Therm. Sci.* **2020**, *29*, 884–892. [CrossRef]
6. Ross, H.D. Ignition of and flame spread over laboratory-scale pools of pure liquid fuels. *Prog. Energy Combust. Sci. Technol.* **1994**, *20*, 17–63. [CrossRef]
7. Chao, C.Y.H.; Wang, J.H.; Kong, W. Effects of fuel properties on the combustion behavior of different types of porous beds soaked with combustible liquid. *Int. J. Heat Mass Transf.* **2004**, *47*, 5201–5210. [CrossRef]
8. Zanganeh, J.; Moghtaderi, B.; Ishida, H. Combustion and flame spread on fuel-soaked porous solids. *Prog. Energy Combust. Sci.* **2013**, *39*, 320–339. [CrossRef]
9. Ishida, H. Flame spread over ground soaked with highly volatile liquid fuel. *Fire Saf. J.* **1988**, *13*, 115–123. [CrossRef]
10. Kong, W.; Chao, C.Y.; Wang, J. Burning characteristics of non-spread diffusion flames of liquid fuel soaked in porous beds. *J. Fire Sci.* **2002**, *20*, 203–225. [CrossRef]
11. Li, M.; Lu, S.; Guo, J.; Chen, R.; Tsui, K.-L. Initial fuel temperature effects on flame spread over aviation kerosene in low-and high-altitude environments. *Fire Technol.* **2015**, *51*, 707–721. [CrossRef]
12. Fu, Y.; Gao, Z.; Ji, J.; Li, K.; Zhang, Y. Experimental study of flame spread over diesel and diesel-wetted sand beds. *Fuel* **2017**, *204*, 54–62. [CrossRef]
13. Zanganeh, J.; Moghtaderi, B. Effect of fuel soaked time and fuel ratio on the flame spread rate over a porous bed wetted with liquid fuel. *Fire Saf. J.* **2013**, *59*, 151–159. [CrossRef]
14. Suzuki, T.; Kawamata, M.; Hirano, T. Flame spread over fuel soaked sand in an opposed air stream. *Fire Saf. Sci.* **1989**, *2*, 199–208. [CrossRef]
15. Ishida, H. Flame tip propagation with assisted flow along fuel-soaked ground. *J. Fire Sci.* **2011**, *29*, 99–110. [CrossRef]
16. Ishida, H.; Kenmotsu, Y. Flame spread in opposed flow along the ground soaked with high-volatile liquid fuel. *J. Fire Sci.* **2009**, *27*, 285–297. [CrossRef]
17. Zanganeh, J.; Moghtaderi, B. Flame spread over porous sand beds wetted with propenol. *Fire Mater.* **2011**, *35*, 61–70. [CrossRef]
18. Zhang, B.; Zhang, J.; Huang, Y.; Wang, Q.; Yu, Z.; Fan, M. Burning process and fire characteristics of transformer oil: A study focusing on the effects of oil type. *J. Therm. Anal. Calorim.* **2020**, *139*, 1839–1848. [CrossRef]
19. Zhou, B.; Yang, W.; Yoshioka, H.; Chen, T.; Wang, K.; Hao, D.; Jiang, C.; Cui, K. Research on suppression effectiveness of compressed air foam for oil-immersed transformer hot oil fire. *Case Stud. Therm. Eng.* **2023**, *49*, 103272. [CrossRef]
20. Sorte, S.; Salgado, A.; Monteiro, A.F.; Ventura, D.; Martins, N.; Oliveira, M.S. Advancing Power Transformer Cooling: The Role of Fluids and Nanofluids—A Comprehensive Review. *Materials* **2025**, *18*, 923. [CrossRef]
21. Li, L.; Zhai, X.; Wang, J.; Chen, P.; Shi, C. Experimental study on vertical spill fire characteristics of transformer oil under continuous spill condition. *Process Saf. Environ. Prot.* **2021**, *156*, 521–530. [CrossRef]
22. Li, L.; Guo, X.; Lu, R.; Chen, P.; Shi, C. Experimental study on horizontal fire spread characteristics of transformer oil. *J. Energy Resour. Technol.* **2022**, *144*, 012107. [CrossRef]
23. Huang, Y.; Guo, Y.; Shang, F.; Zhang, J. Effect of oil immersion on the horizontal flame spread over transformer insulating paperboard with different sizes. *Case Stud. Therm. Eng.* **2025**, *70*, 106076. [CrossRef]
24. Otsu, N. A threshold selection method from gray-level histograms. *IEEE Trans. Syst. Man Cybern.* **1979**, *9*, 62–66. [CrossRef]
25. Li, M.; Shu, Z.; Yi, L.; Chen, B.; Zhao, Y.; Geng, S. Combustion behavior and oscillatory regime of flame spread over ethanol aqueous solution with different proportions. *Fuel* **2019**, *253*, 220–228. [CrossRef]

26. Zhao, K.; Wang, Z.; Ma, S.; Ju, X.; Guo, P.; Cao, X. Experimental study on the diffusion burning and radiative heat delivery of two adjacent heptane pool fires. *Int. J. Therm. Sci.* **2022**, *171*, 107246. [CrossRef]
27. Bergman, T.L. *Fundamentals of Heat and Mass Transfer*; John Wiley & Sons: Hoboken, NJ, USA, 2011.
28. Zhao, K.; Zhou, Y.; Li, S.; Lin, Z. Experimental and numerical study on the burning and opposed flame spread behaviors over PMMA under different flow conditions. *Int. Commun. Heat Mass Transf.* **2025**, *165*, 108989. [CrossRef]
29. Zhang, Y.; Chen, C.; Jiao, W.; Lu, T. Experimental study on burning characteristic of liquid fuel immersed in porous media bed: Effect of particle gradation. *Fuel* **2023**, *344*, 128103. [CrossRef]
30. Gao, S.; Zhu, G.; Gao, Y.; Zhou, J. Experimental study on width effects on downward flame spread over thin PMMA under limited distance condition. *Case Stud. Therm. Eng.* **2019**, *13*, 100382. [CrossRef]
31. Zhao, K.; Zhou, X.; Liu, X.; Lu, L.; Wu, Z.; Peng, F.; Ju, X.; Yang, L. Prediction of Three-Dimensional Downward Flame Spread Characteristics over Poly (methyl methacrylate) Slabs in Different Pressure Environments. *Materials* **2016**, *9*, 948. [CrossRef]
32. Wu, Z.; Peng, M.; Chai, G.; Zhou, J.; Zhou, Y.; Zhu, G. Experimental study on the influence of restricted distance on the discrete flame spread of different widths. *Case Stud. Therm. Eng.* **2024**, *54*, 103973. [CrossRef]
33. Tu, K.-M.; Quintiere, J.G. Wall flame heights with external radiation. *Fire Technol.* **1991**, *27*, 195–203. [CrossRef]
34. Zhao, K.; Yang, L.; Tang, W.; Liu, Q.; Ju, X.; Gong, J. Effect of orientation on the burning and flame characteristics of PMMA slabs under different pressure environments. *Appl. Therm. Eng.* **2019**, *156*, 619–626. [CrossRef]
35. Gollner, M.; Williams, F.; Rangwala, A. Upward flame spread over corrugated cardboard. *Combust. Flame* **2011**, *158*, 1404–1412. [CrossRef]
36. Hu, L. A review of physics and correlations of pool fire behaviour in wind and future challenges. *Fire Saf. J.* **2017**, *91*, 41–55. [CrossRef]
37. Heskestad, G. Luminous heights of turbulent diffusion flames. *Fire Saf. J.* **1983**, *5*, 103–108. [CrossRef]
38. Jeong, J.-J.; Mizuno, M.; Park, K.-W.; Lim, H.-J.; Cho, C.-G. Fire properties of bed mattresses focusing on the fire growth rate and flame height. *Materials* **2022**, *15*, 3757. [CrossRef]
39. Huang, X.; Ding, H.; Zhang, X.; Li, X.; Wang, M.; Zhang, P. Effects of wind speed, spacing distance and heat release rate on the combustion and flame merging characteristics of two extra-thin line fires. *Case Stud. Therm. Eng.* **2024**, *60*, 104676. [CrossRef]
40. Jiang, L.; Miller, C.H.; Gollner, M.J.; Sun, J. Sample width and thickness effects on horizontal flame spread over a thin PMMA surface. *Proc. Combust. Inst.* **2016**, *36*, 2987–2994. [CrossRef]
41. Zhang, Y.; Zhang, D.; Mao, S.; Wang, X.; Lu, K.; Li, B. Experimental study on burning characteristic of liquid fuel-immersed porous media bed in cross airflow. *Int. J. Therm. Sci.* **2025**, *210*, 109677. [CrossRef]
42. Zhang, Y.; Ji, J.; Li, J.; Sun, J.; Wang, Q.; Huang, X. Effects of altitude and sample width on the characteristics of horizontal flame spread over wood sheets. *Fire Saf. J.* **2012**, *51*, 120–125. [CrossRef]